



Photometric program on the 70-centimeter telescope at AGO Modra

Bezovec 2020



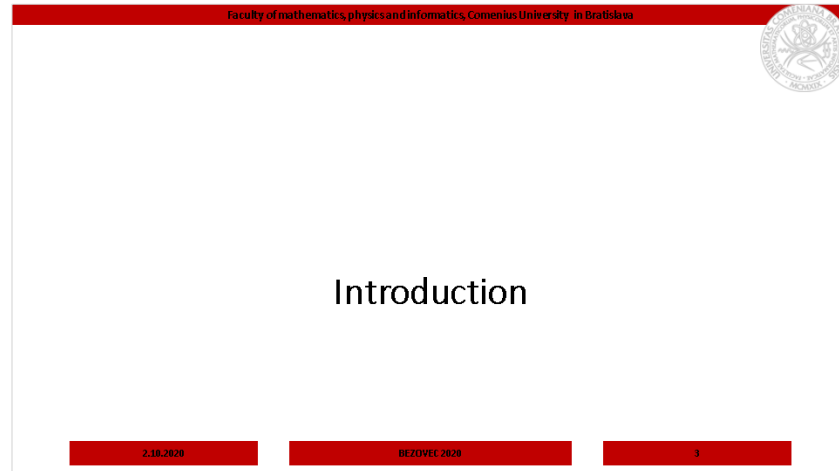
**Matej Zigo, Jiří Šilha, Stanislav Krajčovič,
Tomáš Hrobár**

Faculty of Mathematics, Physics and Informatics,
Comenius University in Bratislava, Slovakia

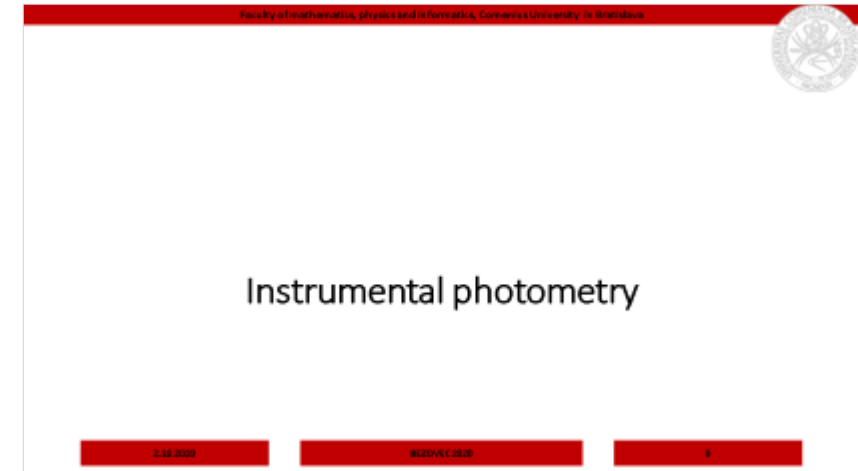


Content

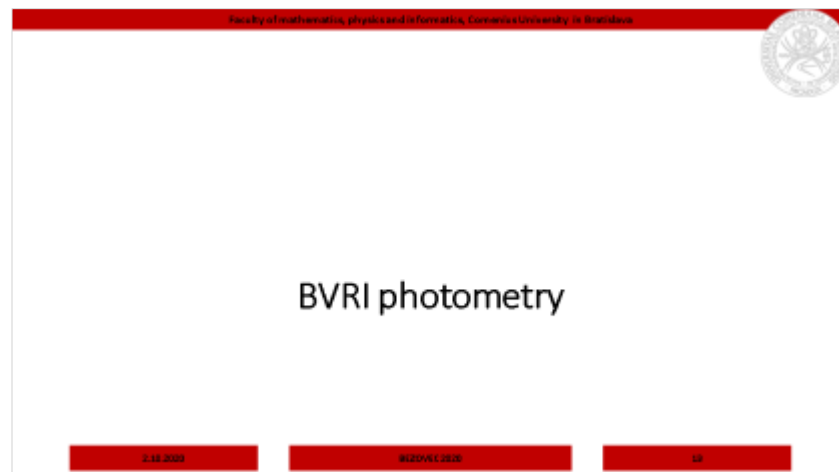
1.



2.



3.



4.



2.10.2020

BEZOVEC 2020

2



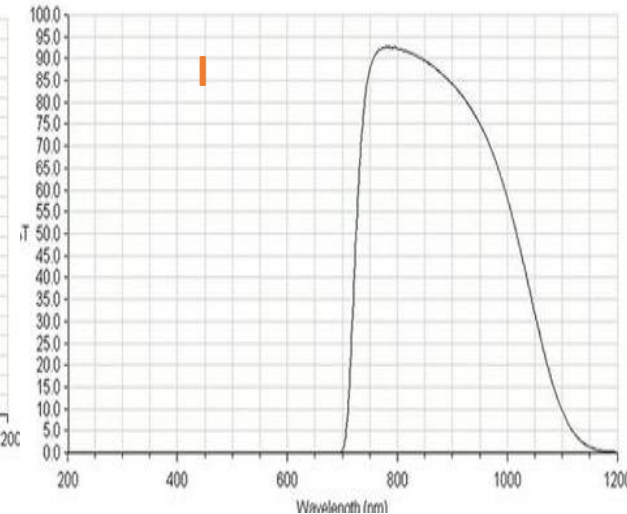
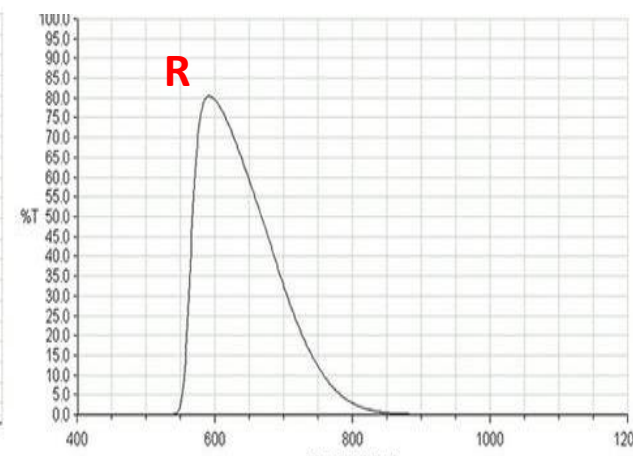
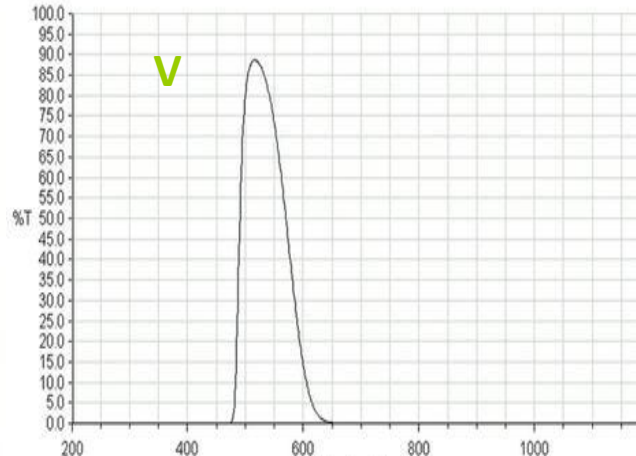
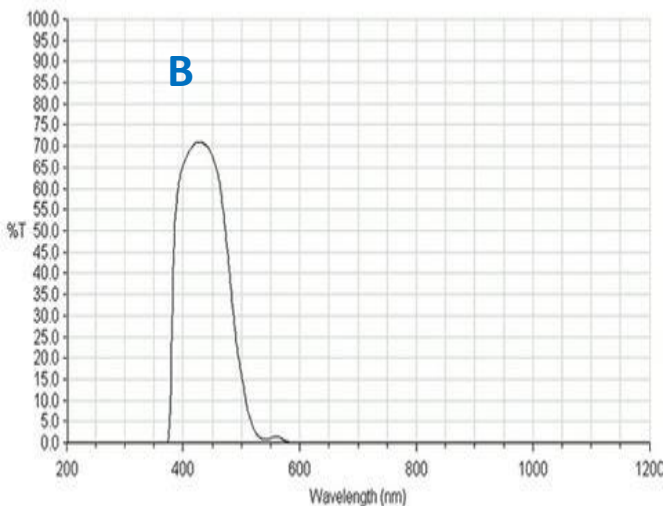
Introduction

AGO 70

- Newtonian telescope
 - fork equatorial mount
 - 0.7m parabolic mirror - focal length – 2.9m
 - main specialization – observations of space debris objects
 - CCD FLI Proline PL1001 Grade 1, 1024 x 1024 pixels
 - iFOV = 1.67"x1.67" and FOV = 28.5'x28.5'
- Johnson – Cousin's filters BVR_I
 - B (435.3nm), V (547.7nm), R (634.9nm), I (879.7nm) ([aip \(2018\)](#))



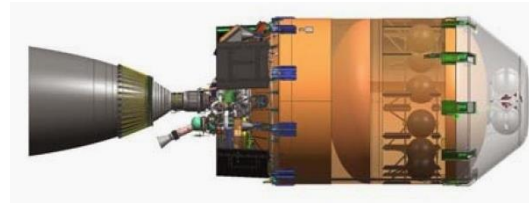
Credit: Stanislav Griguš



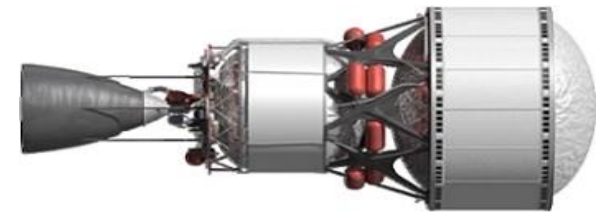
Transmission of Johnson-Cousin Filters installed on AGO 70. Source: [Cloudbreak optics \(2019\)](#)

Objects of interest

- all non-functional, human-made objects, including fragments and elements thereof, in Earth orbit or re-entering into Earth's atmosphere (ESA definition)



Upper stage Falcon 9



Upper stage Delta

Upper stages Breeze-m



Astra satellites



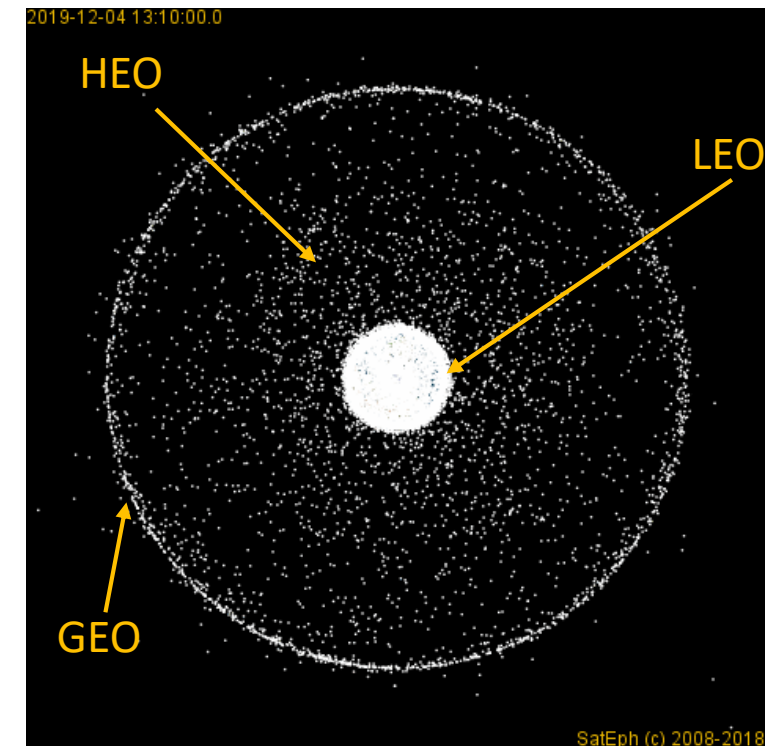
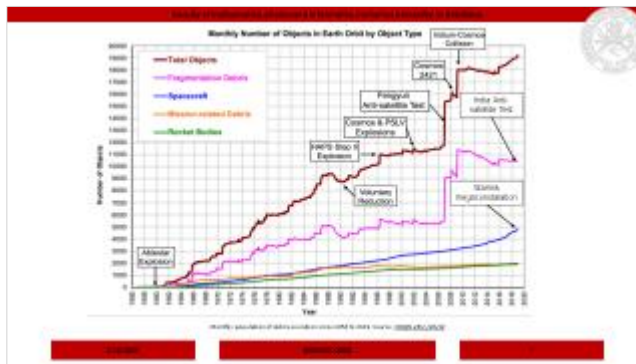
Molniya satellite



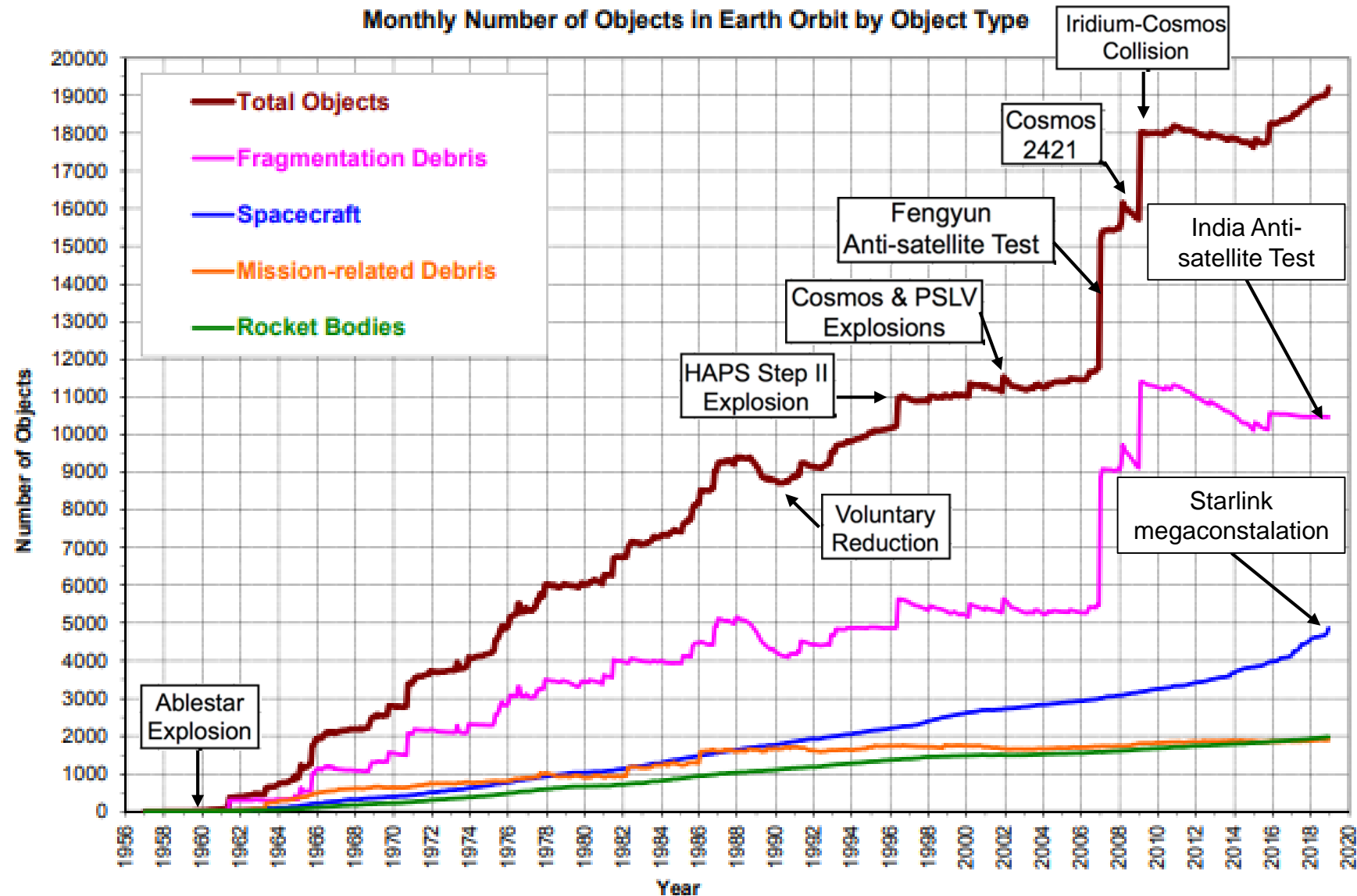
Al₂O₃

Motivation of space debris research

- Increasing population of fragments on all orbits
- Planning active debris removal missions
- Safety of new released missions
- Early warning systems for existing satellites
- Object's identification and characterization
- Looking up for its ancestry



Actual motion of 18399 space debris objects on orbits. Source: SatEph



Monthly population of debris evolution since 1956 to 2019. Source: [ODQN 23i1 \(2019\)](#)

AGO 70

Astrometry

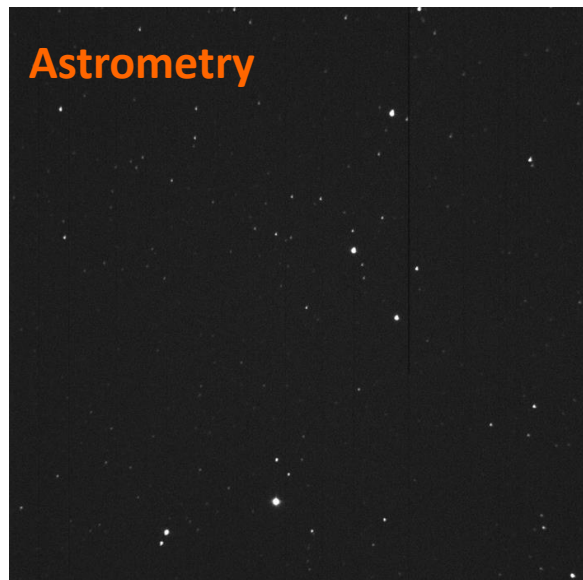


Figure – Images acquired by AGO 70cm telescope. Astrometric observations of satellite IRNSS-1A (13034A). Other four GEO satellites crossing the FOV. Used exposure time of 0.2 s.

Light curves

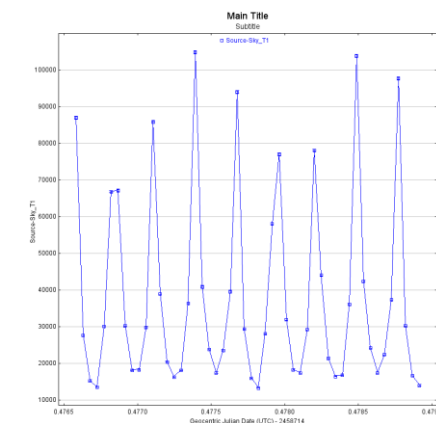
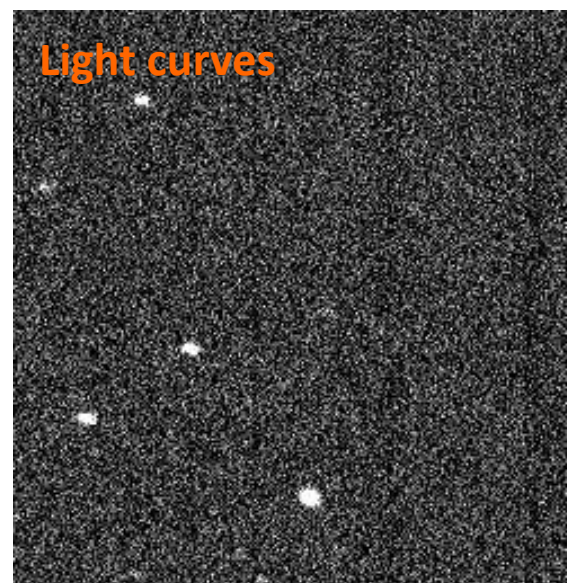


Figure – Object Falcon 9 (19009C) acquired by the AGO 70cm telescope (left) and its constructed light curve from AIJ(right).

BVRI photometry

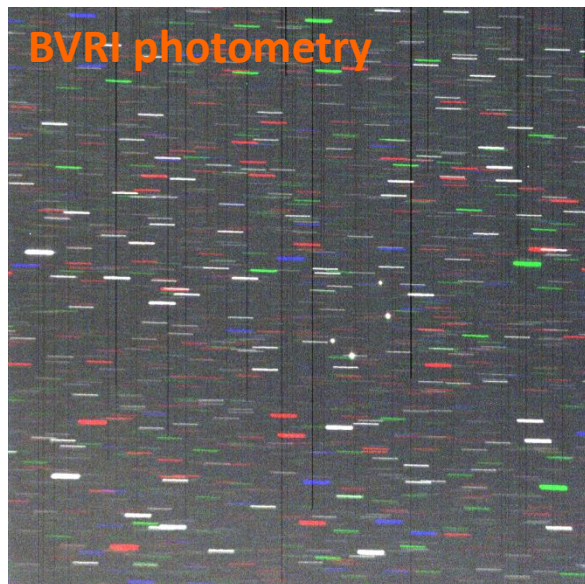


Figure – RVI images acquired by AGO 70cm telescope. Color photometry observations of ASTRA Cluster. Used exposure time of 5.0 s.

LEO tracking support



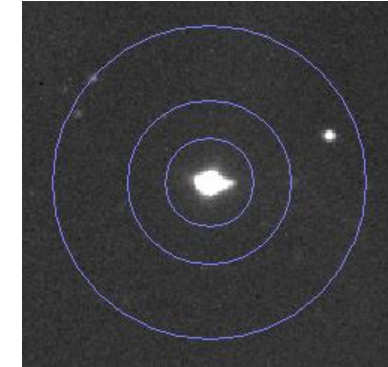
Figure – SL-12 R/B(2) (02037D) observed by AGO 70cm. Compilation of 9 frames, exp = 0.1s, filter I.



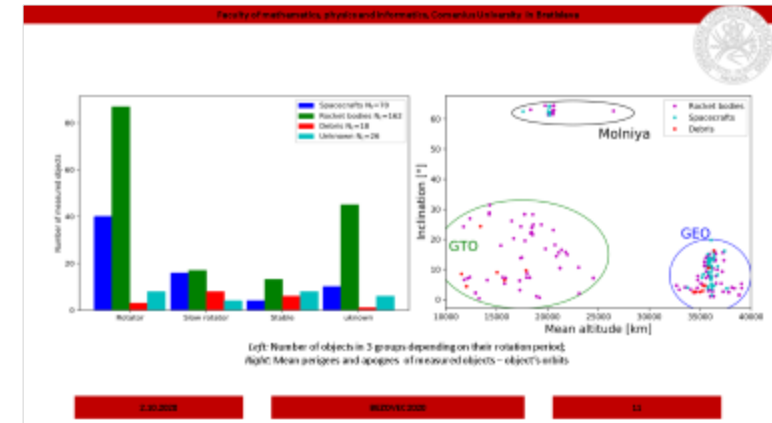
Instrumental photometry

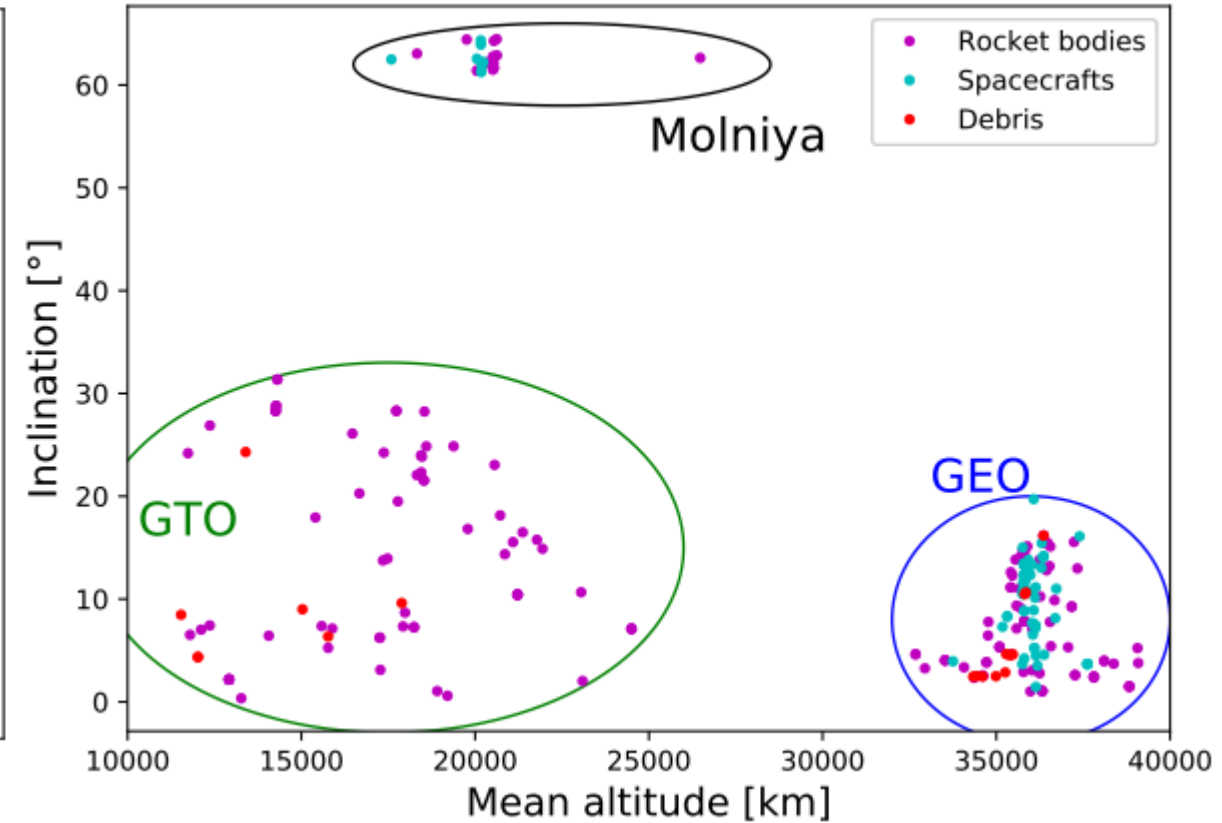
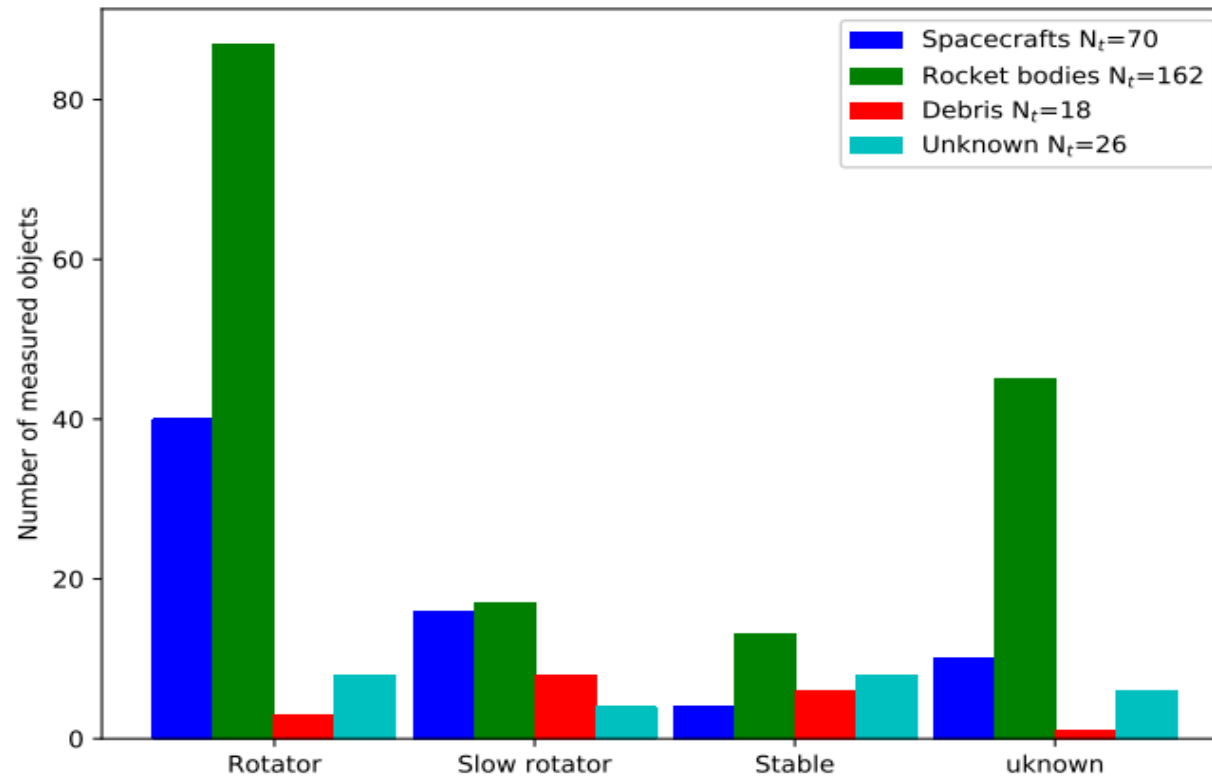
FMPI's Light Curve Catalog

- Aperture photometry program
- Instrumental intensity– acquired using the AstrolmageJ (AIJ)
- Light curves – time dependence of intensity
 - Light curve processing (Hamara dissertation thesis, (2017))
 - Apparent rotation periods – FFT and Lomb Scargle method (Feigelson and Babu, 2017)
 - Phase function – "Phase Dispersion Minimization (PDM)" (Stellingwerf ,1978)
 - Internal database of light curves and phase functions
 - 285 light curves of 226 objects up to the end of March 2019 (Šilha et al., 2020)
- Target selection
 - Any visible object – altitude > 30 deg
 - Building up the catalog for next research

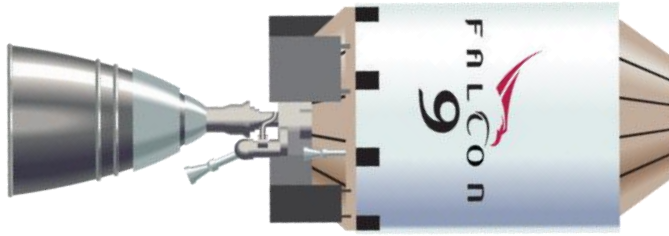


Illustrative screenshot of
AIJ aperture





Left: Number of objects in 3 groups depending on their rotation period;
Right: Mean perigees and apogees of measured objects – object's orbits

Falcon-9 stage 2. Source: [VENGAGE](#)

2017-063B

17063B

94.6

10-Jun-2018 22:18:20

Details

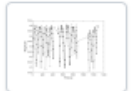


17063B

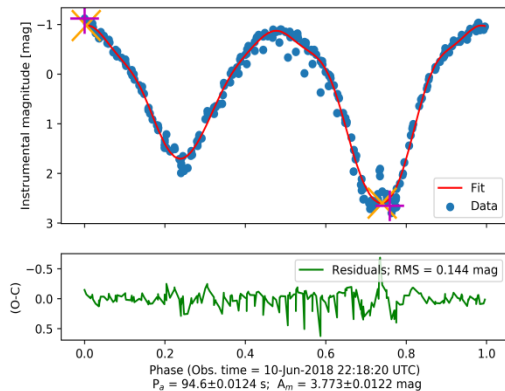
94.7

11-Jun-2018 20:40:25

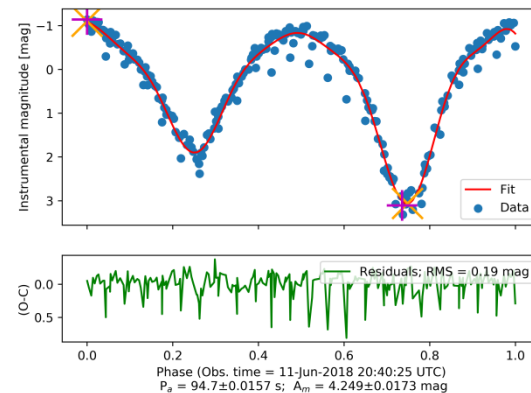
Details



17063B_2_3_4_R_20180610



17063B_2_3_4_R_20180611



Object name: FALCON 9 R/B
COSPAR: 17063B
Object type: rocket body
NORAD: 42968
Orbital period: 619.40
Inclination [deg]: 28.29
Perigee [km]: 205
Apogee [km]: 35179
Decayed: false

Source LC
Period [sec]: 94.6
Period error [sec]: 0.012393
Amplitude [mag]: 3.773
Amp. error [mag]: 0.01225
Number of points: 277
Exposure [sec]: 1.0996
Mean samp. [sec]: 4.6659
Filter: R

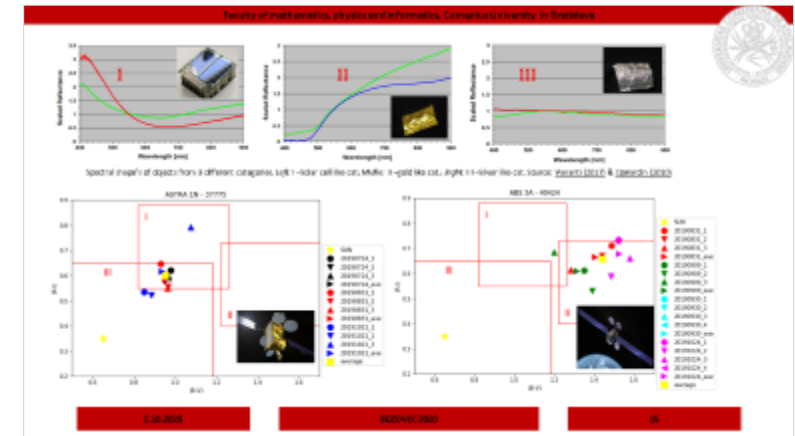
Report of Falcon's 9 rocket body from FMPI's internal catalog. Source: Screen shot of Screenshot of public catalogue (Silha et al., 2020)

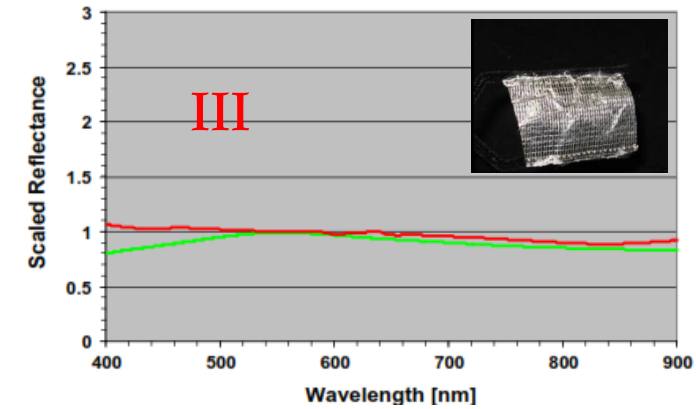
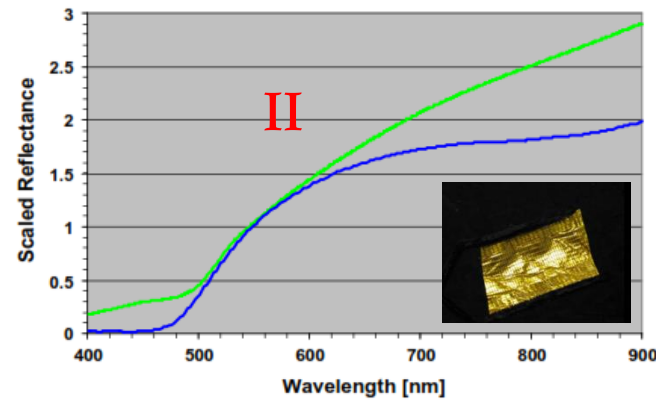
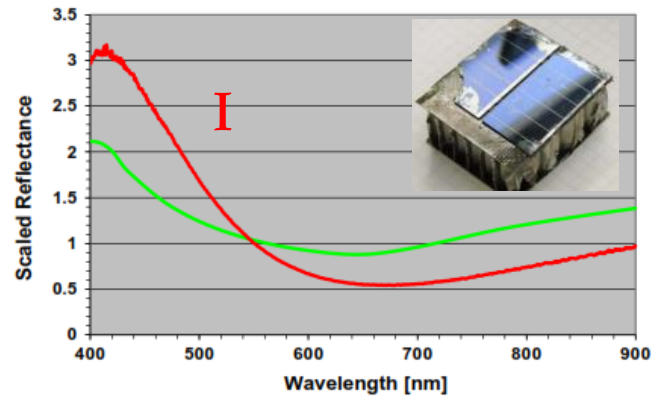


BVRI photometry

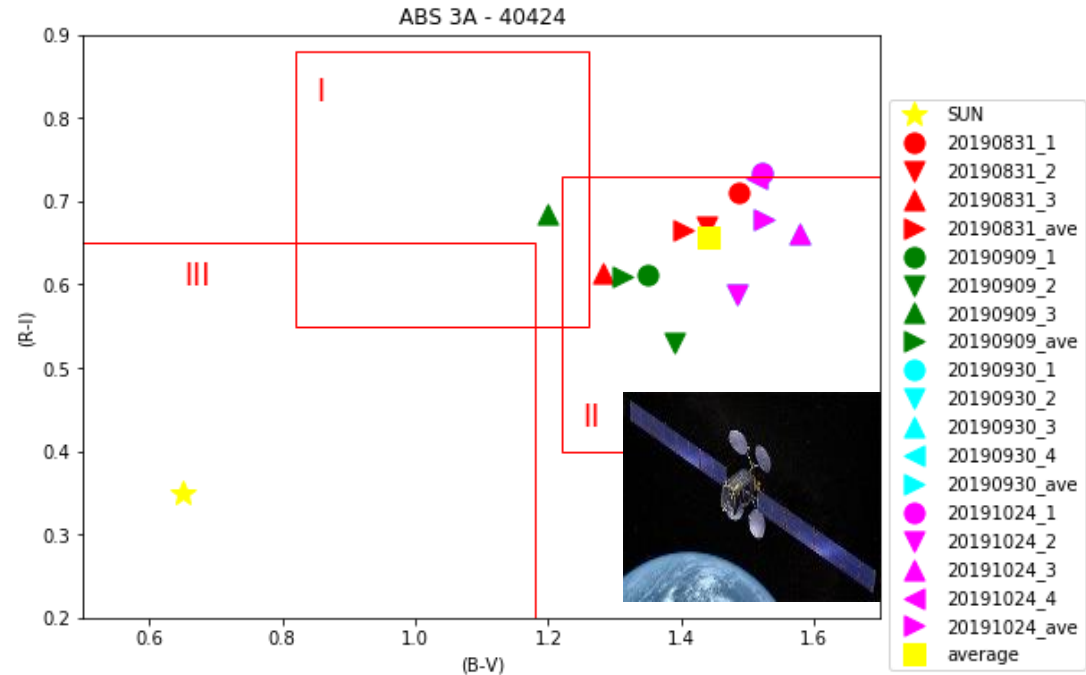
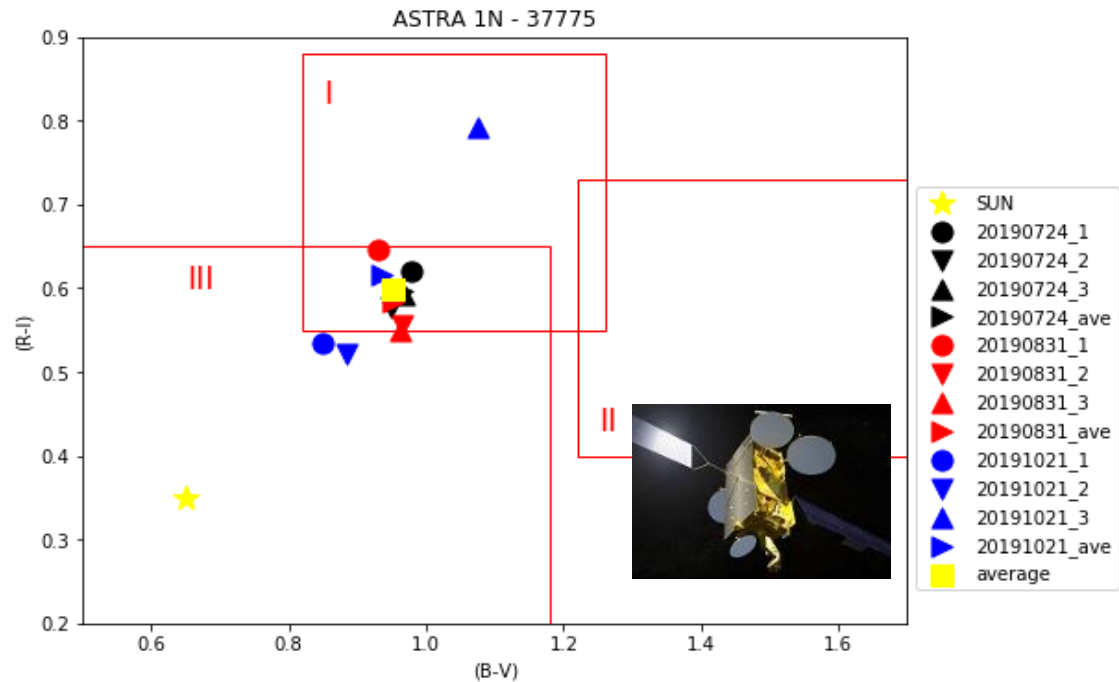
BVRI photometry

- Absolute photometry in BVRI filters
 - Instrumental intensity transformed to standard system of magnitudes
 - Transformation using standard stars
 - Requires good weather conditions and high source SNR(≈ 40)
- Color index – numerical expression of object's color
 - Depends on phase angle
 - Difference of brightness in two filters - B-V, V-R, R-I, V-I,
 - Detected color index depends on object's surface properties
 - Sorting objects into 3 groups according to shape of spectra (Vananti (2017))
 - I - relatively flat with possible negative slope in blue range – solar cell similarities
 - II - monotonic increasing with concave up shape– gold similarities
 - III- monotonic increasing with concave down shape – silver similarities
 - Aging of objects and spaceweathering effects





Spectral shape's of objects from 3 different categories. *Left:* I –Solar cell like cat; *Middle:* II –gold like cat.; *Right:* III –Silver like cat. Source: [Vananti \(2017\)](#) & [Cowardin \(2010\)](#)



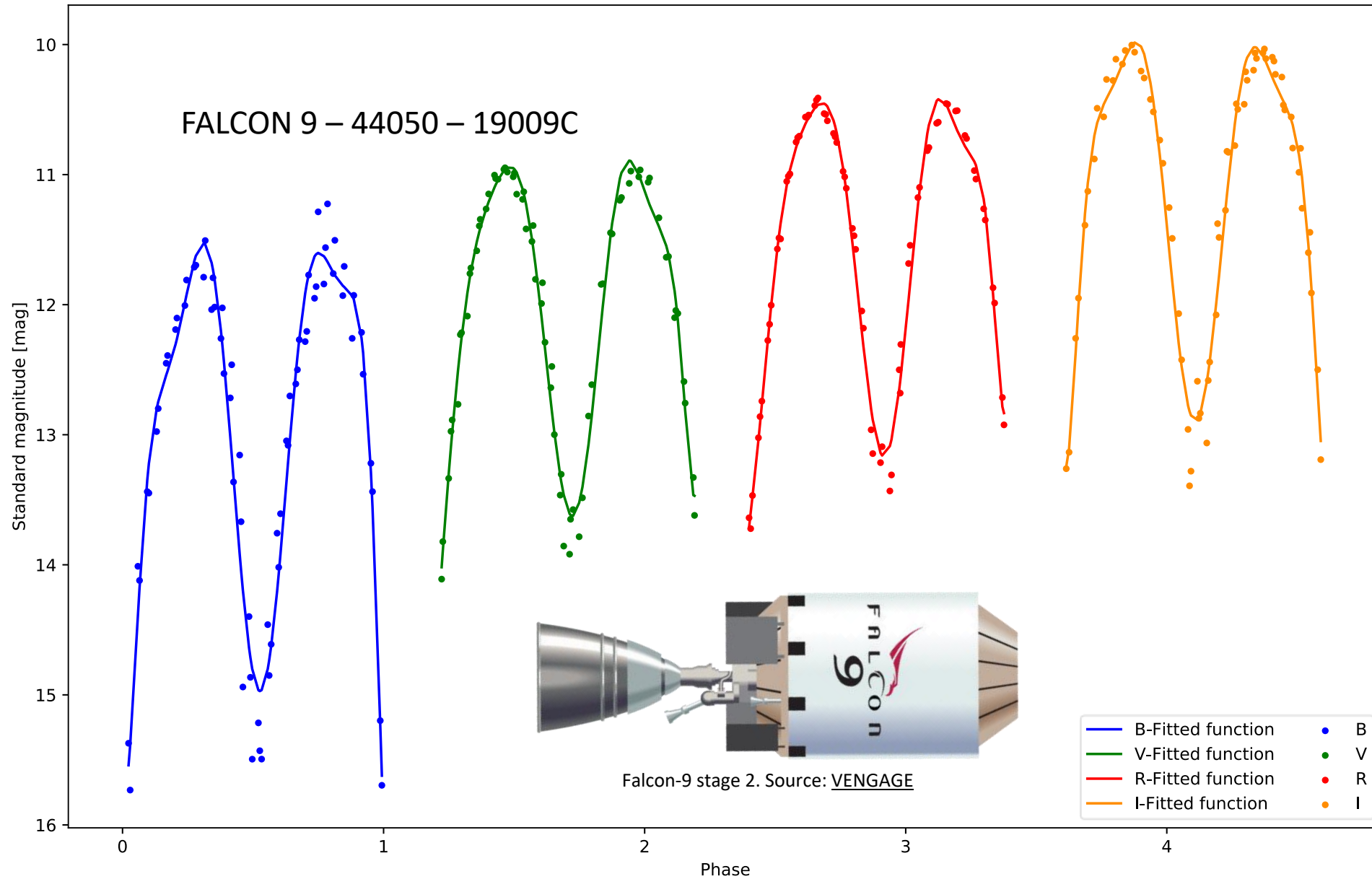


Phase dependence of the color indices

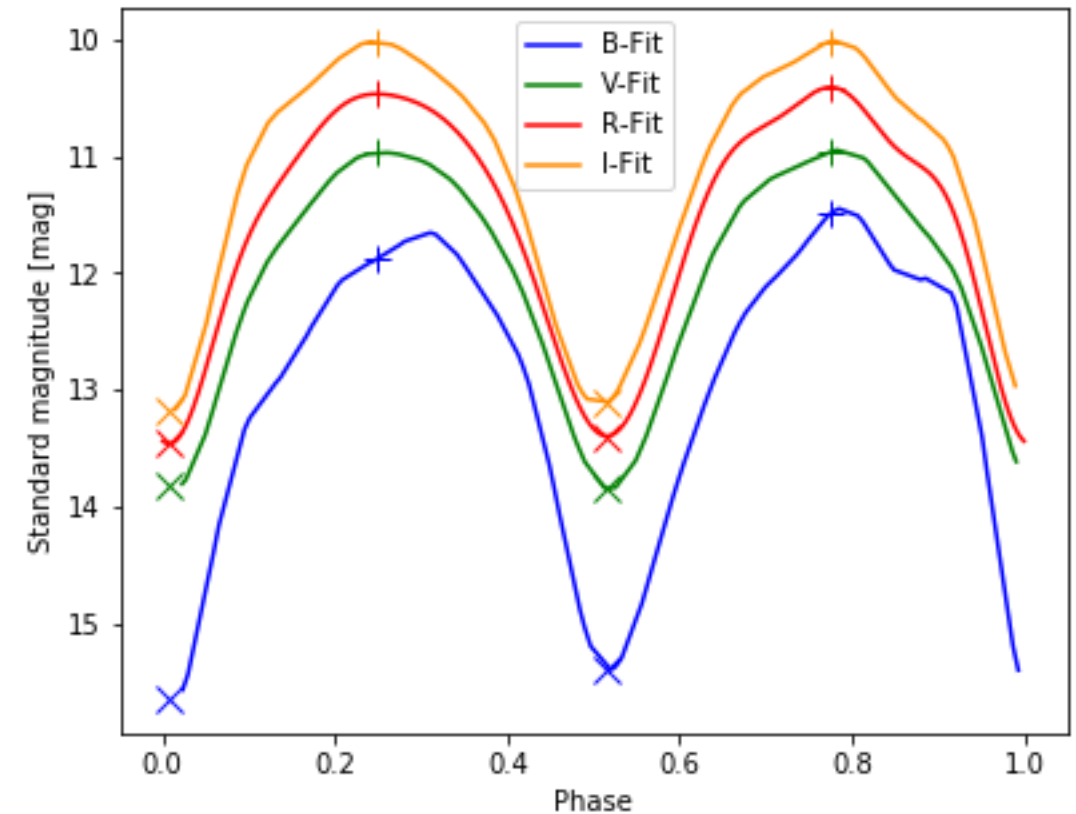
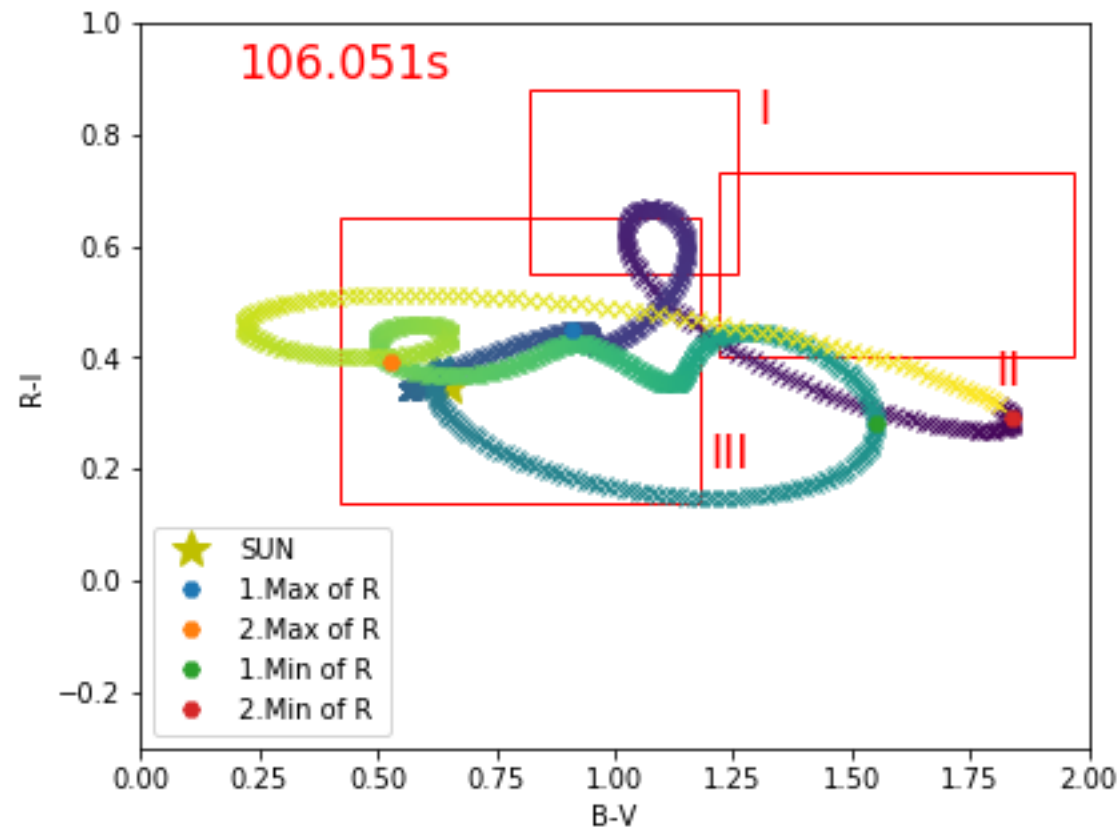
- From pre-processed data is extracted the light curves in each passband
- Phase is reconstructed using the *LCprocessing.m* (Hamara, 2017) simultaneously for each filter
- Estimated period is used for phase construction using formula $t_{phase} = \frac{t-t_0}{P} - \left\lfloor \frac{t-t_0}{P} \right\rfloor$
- The phase functions are then optimized using the Fourier series of 8th degree

$$m = a_0 + \sum_{i=1}^8 [a_i \cdot \cos(i \cdot t_{phase}) + b_i \cdot \sin(i \cdot t_{phase})]$$

- Where a_i, b_i are free parameters, which are optimized
- Fourier fit is inspired by the dissertation thesis (Világi, 2007)
- Then the phase is softened and color indices along the phase are calculated



BVRI diagram of the Max/Min of R filter - object 44050_5





Development

Low-Earth orbit object tracking

- New telescope control unit developed by FMFI
- Polar and declination axis are operated separately
- Maximum tracking speed for both axis is around 5400 arcsec/sec
- Sensor able to monitor all objects higher than 800km
 - Space debris (range > 800 km);
 - Near-Earth objects;
 - Close-Encounters (e.g. NEA with range < 0.1 Lunar Distance km);

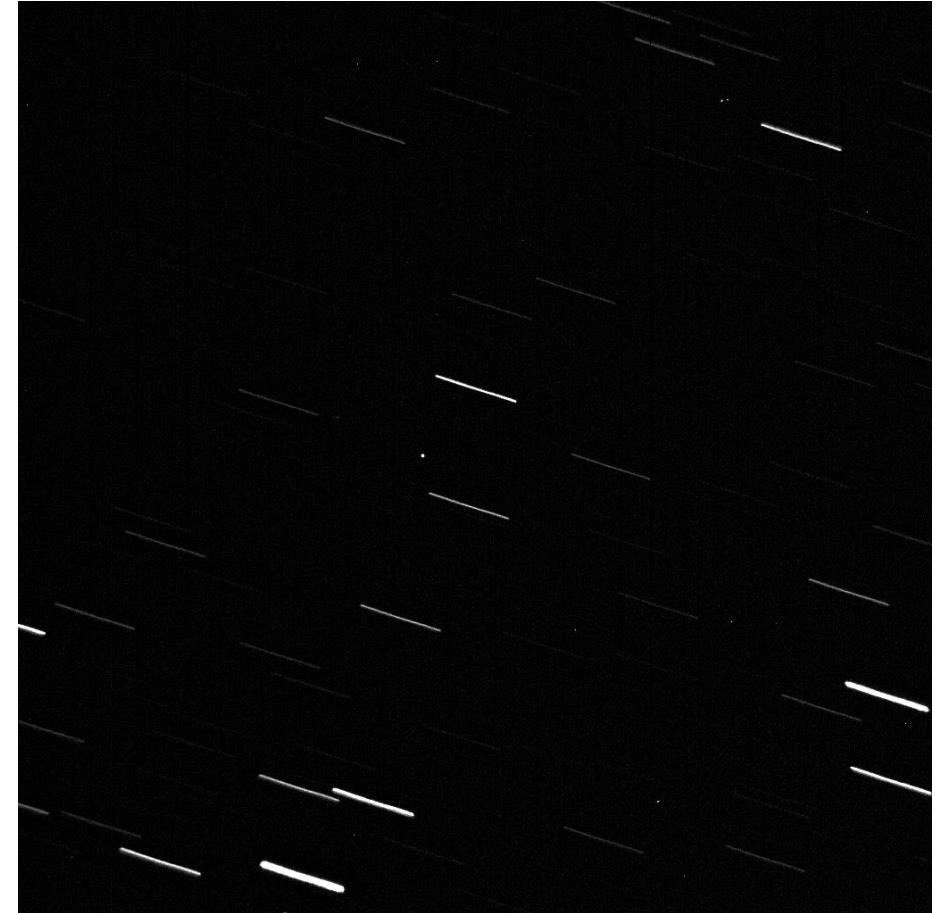


Image processing system

Sidereal tracking



Object tracking

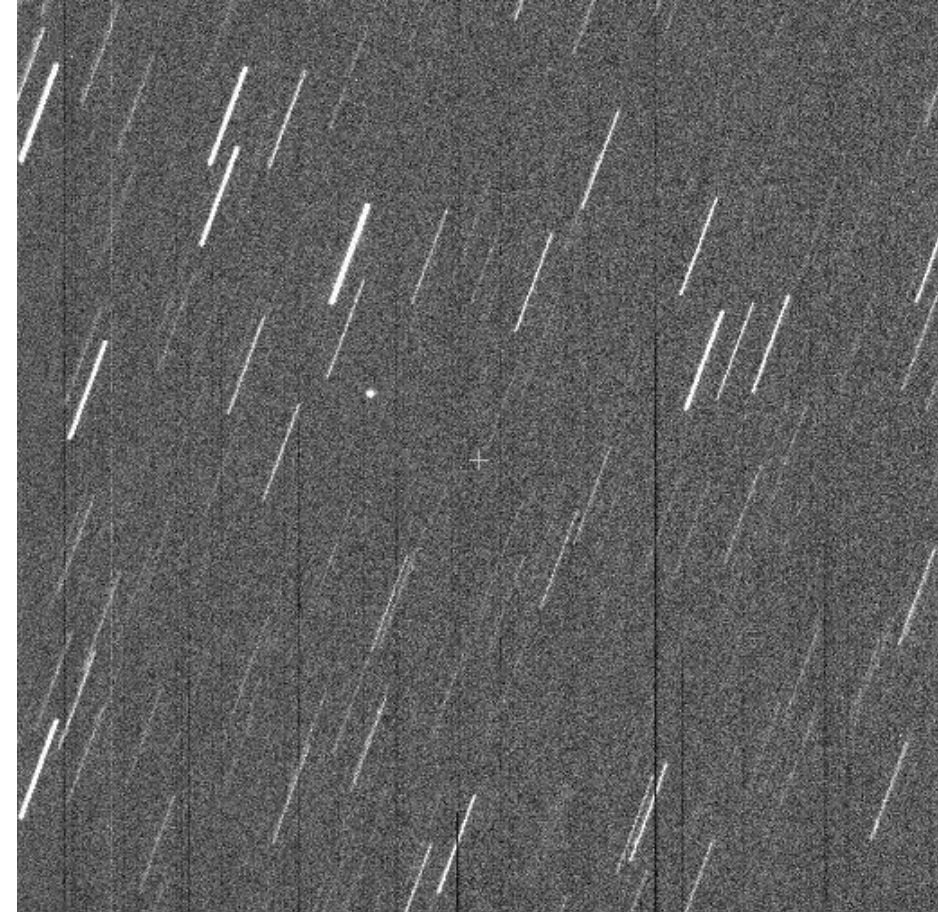
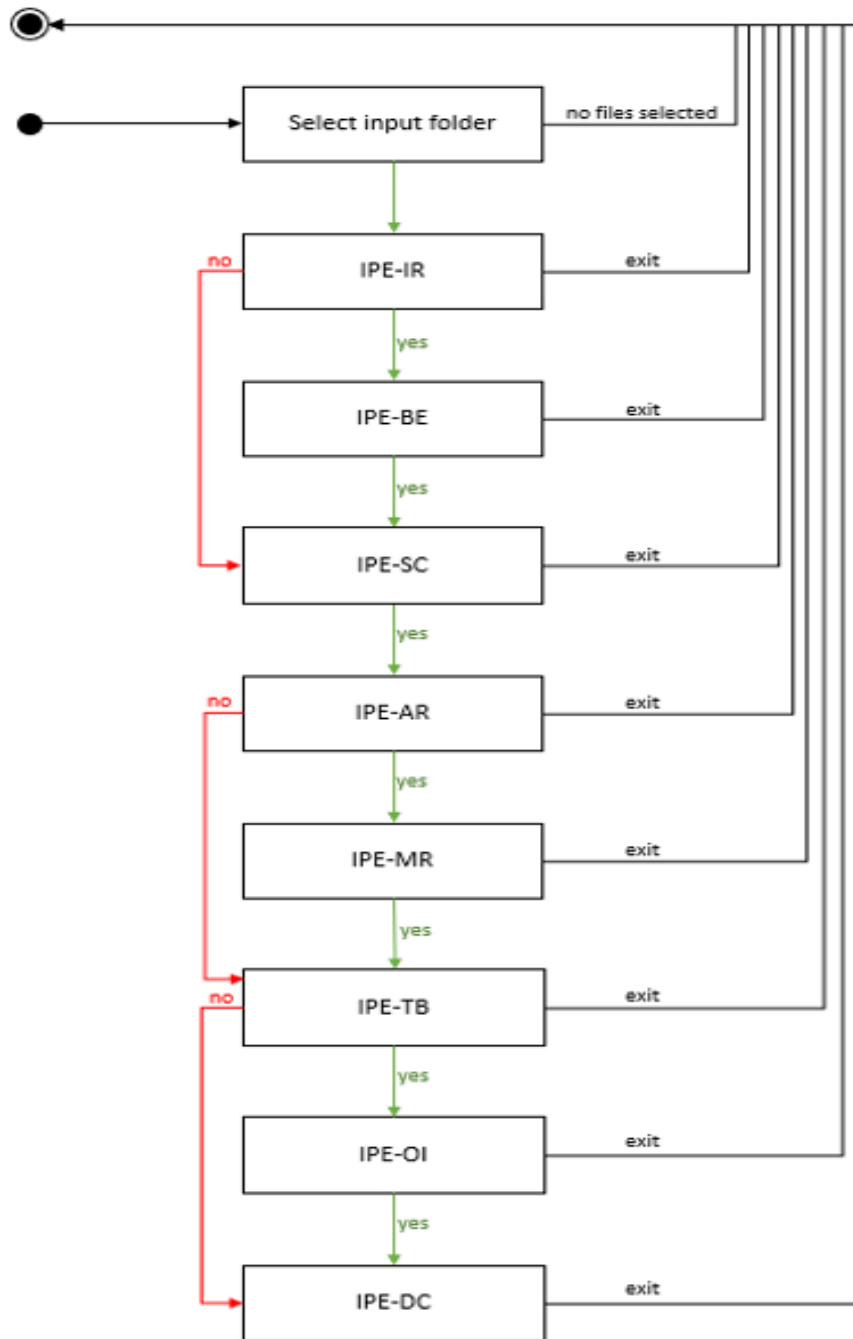


Image processing system

- Modular image processing system
- Each component can be run separately
- Motivation: fast processing of raw images to object's tracklet for TLE improvement
- IPS contains:
 - Casual image calibration
 - Background extraction
 - Search and Centroiding
 - Astrometric reduction
 - Masking
 - Tracklet building
 - Object identification
 - Data conversion





Conclusion

- We presented the current state of the 70-centimeter telescope at AGO
- Instrumental photometry – processing, light curve database
- BVRI photometry – long-term monitoring of average color index, phase dependency of the color index
- Further development of object tracking and image processing system
- An observational campaign has started for calibration and validation of the sensor



Thank you for attention !



References

- ESA FAQ: https://www.esa.int/Safety_Security/Space_Debris/FAQ_Frequently_asked_questions
- *ODQN 23i1 (2019) source*: <https://orbitaldebris.jsc.nasa.gov/quarterly-news/pdfs/odqnv23i1.pdf>
- *Cloudbreaks optics (2019)*: <https://cloudbreakoptics.com/products/50mm-square-ubvri-filters>
- *Aip (2017)*: <https://www.aip.de/en/research/facilities/stella/instruments/data/johnson-ubvri-filter-curves>
- ŠILHA, Jiří, et al. Space debris observations with the Slovak AGO70 telescope: Astrometry and light curves. Advances in Space Research, 2020.
- WARNER, Brian D. a Alan W. HARRIS. A practical guide to lightcurve photometry and analysis. New York: Springer, c2006. ISBN 0-387-29365-5.
- Vananti, A., Schildknecht, T., & Krag, H. (2017). Reflectance spectroscopy characterization of space debris. Advances in Space Research, 59(10), 2488-2500. doi:10.1016/j.asr.2017.02.033
- HAMARA, M.; Rotation properties of the artificial objects in the vicinity of Earth; Dissertation Thesis; Comenius University in Bratislava; Faculty of Mathematics, Physics and Informatics Bratislava 2017, Retrieved from <http://opac.crzp.sk/?fn=detailBiblioForm&sid=F065241B7212E93A23176233722A&seo=CRZP-detail-kniha>
- SILHA J., HAMARA M., "Color Indices of Selected Objects Situated on the MEO and GEO Orbits Obtained by two Telescopes Observations", Proceedings of 6th European Conference on Space Debris, Darmstadt, Germany, 2013
- COWARDIN, H.M.: CHARACTERIZATION OF ORBITAL DEBRIS OBJECTS OVER OPTICAL WAVELENGTHS VIA LABORATORY MEASUREMENTS; Dissertation Thesis; University of Houston; the Faculty of the Department of Physics Houston May 2010
- FEIGELSON, E. D.; BABU, G. J. 2012. Modern Statistical Methods for Astronomy. Cambridge University Press. ISBN: 978-0-521-76727-9, s. 292
▪ 36